Properties of GluR3 receptors tagged with GFP at the amino or carboxyl terminus

Agenor Limon*, Jorge Mauricio Reyes-Ruiz*, Fabrizio Eusebi†, and Ricardo Miledi*‡§

*Department of Neurobiology and Behavior, University of California, Irvine, CA 92697-4550; †Dipartimento di Fisiologia Umana & Farmacologia, Universita' di Roma ''Sapienza,'' and Neuromed Via Atinese 18, I86077 Isernia, Italy; ‡Instituto de Neurobiología, Laboratorio de Neurobiología Molecular y Celular, Universidad Nacional Autónoma de México, Campus Juriquilla, Boulevard Juriquilla 3001, Juriquilla, Querétaro, 76230, México

Contributed by Ricardo Miledi, July 25, 2007 (sent for review May 6, 2007)

Anatomical visualization of neurotransmitter receptor localization is facilitated by tagging receptors, but this process can alter their functional properties. We have evaluated the distribution and properties of WT glutamate receptor 3 (GluR3) α-amino-3-hydroxy-5-methyl-4-isoxazole propionic acid (AMPA) receptors (WT GluR3) and two receptors in which GFP was tagged to the amino terminus (GFP-GluR3) or to the carboxyl terminus (GluR3-GFP). Although the fluorescence in *Xenopus* oocytes was stronger in the vegetal hemisphere because of localization of internal structures (probable sites of production, storage or recycling of receptors), the insertion of receptors into the plasma membrane was polarized to the animal hemisphere. The fluorescence intensity of oocytes injected with GluR3-GFP RNA was approximately double that of oocytes injected with GFP-GluR3 RNA. Accordingly, GluR3-GFP oocytes generated larger kainate-induced currents than GFP-GluR3 oocytes, with similar EC_{50} values. Currents elicited by glutamate, or AMPA coapplied with cyclothiazide, were also larger in GluR3-GFP oocytes. The glutamate- to kainate-current amplitude ratios differed, with GluR3-GFP being activated more efficiently by glutamate than the WT or GFP-GluR3 receptors. This pattern correlates with the slower decay of glutamate-induced currents generated by GluR3-GFP receptors. These changes were not observed when GFP was tagged to the amino terminus, and these receptors behaved like the WT. The antagonistic effects of 6-nitro-7-sulfamoylbenzo-[*f*]quinoxaline-2,3-dione (NBQX) and 6-cyano-7-nitroquinoxaline-2,3-dione (CNQX) were not altered in any of the tagged receptors. We conclude that GFP is a useful and convenient tag for visualizing these proteins. However, the effects of different sites of tag insertion on receptor characteristics must be taken into account in assessing the roles played by these receptor proteins.

fluorescent tag | receptor expression | *Xenopus* oocytes | kainate | glutamate

Glutamate is the main excitatory neurotransmitter in the mammalian central nervous system. Its receptors can either link to a second messenger receptor channel-coupling system (metabotropic) or can themselves form ligand-gated ion channels (ionotropic) (1, 2). The ionotropic glutamate receptors are divided into three groups, according to their differential affinity for the agonists *N*-methyl-D-aspartate (NMDA), kainate (Kai), and α-amino-3-hydroxy-5-methyl-4-isoxazole propionic acid (AMPA) (2). Functional AMPA receptors are made up of homomeric or heteromeric arrangements of the glutamate receptor (GluR)-1 to -4 subunits; their membrane topology indicates an extracellular amino terminus, three transmembrane segments, one membrane reentrant loop, and an intracellular carboxyl-terminal end (3, 4). The receptors are localized mainly postsynaptically and play important roles in the development and function of the nervous system (5, 6).

To study the temporal and spatial distribution of receptors, it is very convenient to label them with fluorescent markers, such as the green fluorescent protein (GFP) (e.g., refs. 7–9). Despite the increasing use of fluorescent tagging to visualize receptors and other cellular proteins, there is no report on the functional properties of GFP-tagged AMPA receptors. Whereas GFP tagging does not seem to alter the function of some receptors (10–13), it is known that for some receptors GFP alters their function (14–16), membrane localization (17) or rate of membrane incorporation (18). With this question in mind, we analyzed the properties of homomeric GFP-tagged GluR3 receptors expressed in *Xenopus* oocytes. $GluR3_{flop}$ was chosen because it is one of the most common AMPA receptors in the central nervous system and because it produces functional homomeric receptors that generate large current responses (19).

Results

Visualization of GFP-Tagged GluR3 Receptors. Oocytes injected in their equator with either GluR3-GFP or GFP-GluR3 cloned mRNAs had fluorescent signals that were clearly more intense than the native fluorescence displayed by noninjected oocytes or those injected with wild-type (WT) GluR3 (Fig. 1 *A* and *B*). The increased fluorescence of oocytes injected with the GFP constructs became obvious 2 days after injection and was polarized to the vegetal hemisphere. The fluorescence intensity of GluR3-GFP oocytes was approximately double that of oocytes injected with GFP-GluR3 (see Fig. 3*A*). Closer observation of the oocyte's surface showed that the fluorescence in the vegetal hemisphere was mainly intracellular, located in small patches around cortical granules that were visible as unlabeled round shapes. It was also present in elongated structures situated 5–10 μm below the oocyte's surface that closely resemble the annulate lamellae (20) (Fig. 1 *E–G*). Interestingly, the animal hemisphere also exhibited a punctate fluorescence, which was seen only within 3 μm of the oocyte's surface.

Because the oocytes injected with the GluR3 GFP chimeras showed a stronger fluorescence in the vegetal hemisphere, principally localized beneath the plasma membrane, it was important to determine the distribution of the receptors actually present in the membrane. Immunolabeling the extracellular amino terminus of GluR3 receptors in nonpermeabilized oocytes showed that the membrane incorporation of receptors is more conspicuous in the animal hemisphere than in the vegetal one (Fig. 1 *C* and *D*), indicating that the stronger GFP signal of the vegetal side arises mainly from the structures beneath the oocyte's surface. The presence of WT and chimeric GlurR3 receptors in *Xenopus* oocyte membranes was analyzed by Western blots. An antibody against the extracellular amino terminus of GluR3 recognized the WT GluR3 and the chimeras in

Author contributions: A.L., J.M.R.-R., and R.M. designed research; A.L., J.M.R.-R., and R.M. performed research; F.E. contributed new reagents/analytic tools; A.L., J.M.R.-R., and R.M. analyzed data; and A.L., J.M.R.-R., F.E., and R.M. wrote the paper.

The authors declare no conflict of interest.

Abbreviations: GluR, glutamate receptor; Kai, kainate; Kai-current, kainate induced current; Glu-current, glutamate induced current; AMPA, α-amino-3-hydroxy-5-methyl-4-isoxazole propionic acid; CNQX, 6-cyano-7-nitroquinoxaline-2,3-dione; NBQX, 6-nitro-7-sulfamoylbenzo[*f*]quinoxaline-2,3-dione; CTZ, cyclothiazide; AL, annulate lamellae.

§To whom correspondence should be addressed. E-mail: rmiledi@uci.edu.

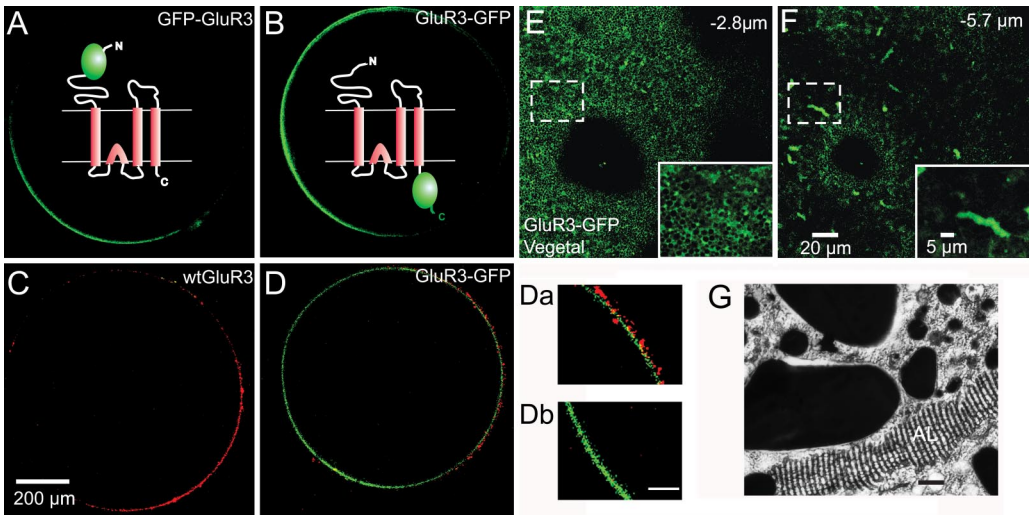

Fig. 1. Visualization of GFP-tagged GluR3. (*A–D*) Confocal sections of oocytes injected in the equator with the indicated cRNAs, taken at 300 μm from the bottom of the oocyte. The animal hemisphere is at the right and the vegetal at the left. Note that the fluorescence is more intense in the vegetal hemisphere. Diagrams in *A* and *B* represent the GluR3 chimeras showing the extracellular or intracellular localization of the GFP. (*C* and *D*) Immunolocalization of GluR3 receptors in the plasma membrane of nonpermeabilized oocytes. (*C*) Oocyte expressing WT GluR3 incubated with an antibody against the amino terminus of GluR3, which is localized extracellularly and a secondary antibody (Alexa 568, red label). (*D*) Oocyte expressing GluR3-GFP incubated with the same primary and secondary antibodies. Note that the insertion of GluR3 is mainly polarized to the plasma membrane in the animal hemisphere. (*Da* and *Db*) Magnification of the membrane near the animal and vegetal poles of the oocyte shown in *D*. (Scale bar: 50 μm.) (*E* and *F*) *Z*-axis sequential scans in the vegetal hemisphere of an oocyte injected with GluR3-GFP. (*Insets*) Magnifications of the areas within the smaller squares. Images taken at 2.8 and 5.7 μm from the oocyte's surface. Below the surface, notice high fluorescence in elongated structures, resembling annulate lamellae. (*G*) Electron microscope image of an annulate lamellae (AL). (Scale bar: 1 μm.) Adapted from R.M. and C. Tate (unpublished work 1978).

Xenopus oocyte membranes. Interestingly, an antiGluR2/3 receptor antibody that is directed against an epitope in the carboxyl terminus of GluR3 recognized both WT and GFP-GluR3 receptors but failed to recognize GluR3-GFP (Fig. 2).

Properties of GFP-Tagged GluR3 Receptors. The functionality of the WT GluR3 and its chimeric receptors was assessed by applying kainate (100 μM), which elicited inward Kai-currents in all of the injected oocytes clamped at -80 mV (Fig. 3*C*). The time course of the Kai-currents was not significantly different between the chimeras and the WT. Currents below $\approx$1.5 μA displayed a smooth activation and reached a fairly steady state; whereas currents greater than $\approx$1.5 μA showed a peak followed by a fast decay and a plateau (Fig. 3*C*).

The peak amplitudes of the Kai-currents were approximately three times larger in oocytes expressing GluR3-GFP than in oocytes expressing WT GluR3 or GFP-GluR3 (Fig. 3*B*); and there was no significant difference between the latter ($n = 64$; $P > 0.5$). Coapplication of 10 μM AMPA plus 10 μM cyclothiazide (CTZ) elicited maintained currents that were also larger in oocytes expressing GluR3-GFP (Fig. 3*D*). To determine whether the chimeras retain the current rectification shown by WT GluR3 receptors at positive membrane potentials (21), slow potential ramps (20 mV/s) from -120 to 60 mV, departing from a V_H of -80 mV, were applied to oocytes expressing the different types of receptors. In all instances the rectification was maintained (data not shown). Application of 1 mM glutamate alone generated much smaller currents (Fig. 4*A*); but here again the GluR3-GFP oocytes elicited larger currents than oocytes expressing WT GluR3 or GFP-GluR3 receptors. When the Glu-currents were compared with Kai-currents in the same oocytes the Glu/Kai-current ratio was greater in the GluR3-GFP oocytes (Fig. 4 *A* and *B*; $n = 106$).

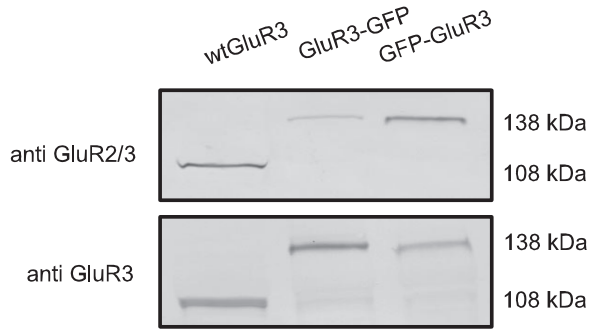

Fig. 2. Differences in antibody selectivity against GluR3 chimeras. Western blots against GluR3 receptors in the membranes of *Xenopus* oocytes in 10% (*Upper*) and 8% (*Lower*) gels. Notice that the anti-GluR2/3 fails to recognize properly the GluR3-GFP.

To better analyze differences in agonist potency and sensitivity, agonist concentration/response curves were constructed for kainate, glutamate and for AMPA coapplied with CTZ to reduce receptor desensitization. The WT GluR3 receptors and the chimeras showed similar kainate concentration/response curves with no statistical difference between their EC_{50}, whereas the n_H values were all different and ranged between 1.2 and 3 (Fig. 5*A* and Table 1). Concentration/response curves for glutamate showed that GluR3-GFP receptors are less sensitive to glutamate than the others. This difference was even greater for AMPA which, in the presence of CTZ, showed less apparent affinity for GluR3-GFP than the other GluR3 receptors (Fig. 5*C*). In addition, the effect of two GluR antagonists was evaluated on currents elicited by 30 μM kainate, applied every 2 min, in oocytes expressing each of the three types of receptors. There was no significant difference in the IC_{50} values for the blocking effects of 6-nitro-7-sulfamoylbenzo[*f*]quinoxaline-2,3-dione (NBQX), or 6-cyano-7-nitroquinoxaline-2,3-dione (CNQX) on the three types of receptors (Fig. 5*D*).

The paradoxical result of smaller glutamate apparent affinity and larger currents generated by the activation of GluR3-GFP, might be partly due to a reduced receptor desensitization. To

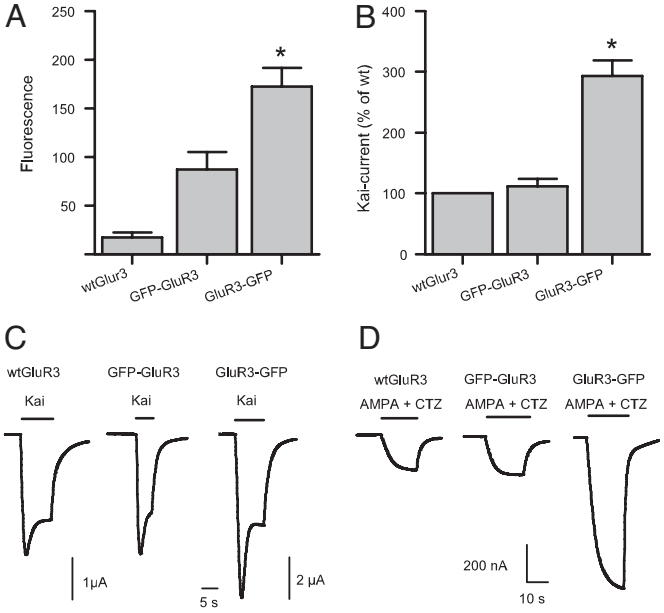

Fig. 3. GluR3 GFP-constructs have different expressional potencies. (*A*) Fluorescence intensity (arbitrary units) of injected oocytes. The fluorescence of oocytes expressing WT GluR3 is the same as the native fluorescence observed in noninjected oocytes ($n = 9$ each). The fluorescence of oocytes expressing GluR3-GFP was double of that of oocytes expressing GFP-GluR3 ($P < 0.05$). (*B*) GluR3-GFP injected oocytes generated nearly three times more 100 μM Kai-current than oocytes injected with WT GluR3 or GFP-GluR3 cRNA ($P < 0.05$; $n = 64$). (*C*) Sample membrane currents evoked by 100 μM kainate in injected oocytes. The 2 μA calibration bar applies only to the GluR3-GFP current. (*D*) The currents elicited by 10 μM AMPA plus 10 μM CTZ were also larger in oocytes expressing the GluR3-GFP.

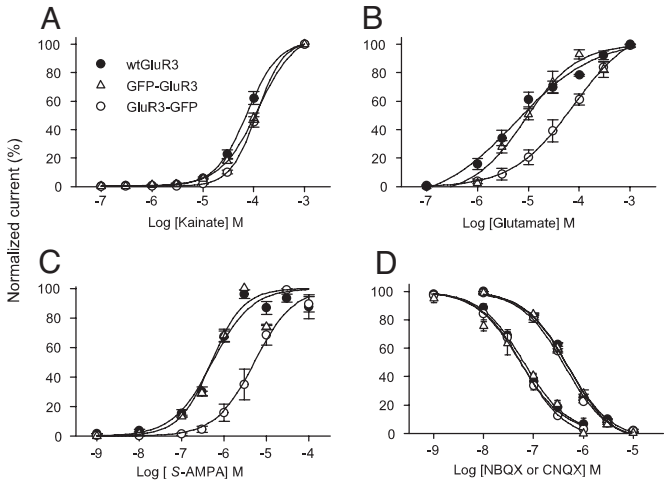

Fig. 5. Agonist and antagonist dose/current response relationships of oocytes expressing GluR3 receptors. (*A*) There was no statistical difference between kainate EC_{50} of WT GluR3, GFP-GluR3 and GluR3-GFP receptors. (*B* and *C*) GluR3-GFP has less sensitivity to glutamate alone, and to AMPA coapplied with 10 μM CTZ than the other GluR3 receptors. (*D*) Neither NBQX (left) nor CNQX (right) concentration/current relationships were altered by GFP tagging to WT GluR3. The action of CNQX and NBQX was evaluated on 30 μM Kai-currents. Currents were normalized to the maximum drug-elicited current for each oocyte ($n = 3$–9).

address this issue the time constant of decay (τ_d) of Glu-currents was analyzed. Application of glutamate plus CTZ, after a brief preapplication of CTZ to inhibit GluR3 desensitization (22), elicited large rapidly activating and inactivating inward currents (Fig. 6*A*). Whereas the time to peak was very similar for all GluR3 receptors, the GluR3-GFP receptors showed a slower τ_d than the other receptors, suggesting changes in the kinetic properties of the receptors ($n = 32$). Even though differences in rates of desensitization may explain the paradoxical behavior of GluR3-GFP, differences in the unitary channel gating and kinetics properties may still be involved.

We also found that potentiation of the 1 mM Glu-current by 10 μM CTZ is smaller in GluR3-GFP oocytes (1,163 ± 325%; $n = 12$) than in GFP-GluR3 (1,872 ± 414%; $n = 13$) and WT GluR3 (2,422 ± 391%; $n = 13$) oocytes. However, this difference was significant only when comparing GluR3-GFP to WT GluR3 receptors, and GFP-GluR3 receptors were not statistically different, probably because of the high variability of the potentiation.

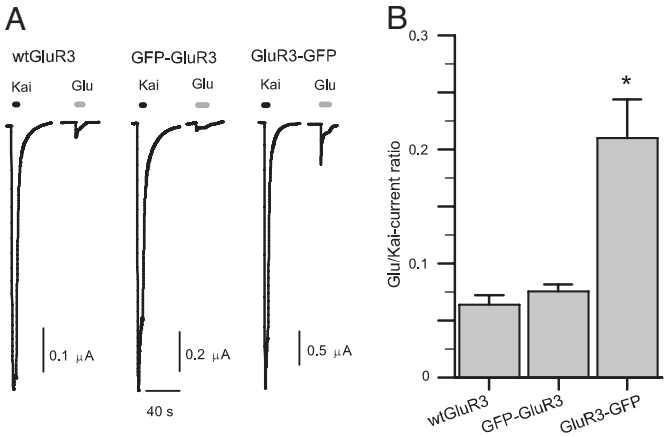

Fig. 4. Glutamate-induced currents are larger in GluR3-GFP oocytes. (*A*) Normalized sample Kai- and Glu-currents generated by the different receptors. Kai was 100 μM and glutamate was 1 mM. (*B*) Glutamate is about three times more efficient in eliciting currents in oocytes injected with GluR3-GFP than in oocytes injected with WT GluR3 or GFP-GluR3 ($n = 106$).

Discussion

Two main findings arose from this study. First, it is clear that the oocyte's fluorescence of GFP tagged receptors does not match strictly the plasma membrane sites containing the receptors. Second, it is evident that, depending on the site of GFP insertion, the tagging can produce substantial changes in the properties of the receptors. Regarding the spatial distribution of the GluR3 chimeras, the overall fluorescence was strongly polarized to the vegetal hemisphere in oocytes injected with either of the two constructs. This localization was unexpected, because it is known that the expression of endogenous and exogenous ionic channels and neurotransmitter receptors is mainly polarized to the animal hemisphere (15, 18, 23–25). However, some potassium channels are expressed at higher levels in the vegetal side (26, 27). Immunolabeling of the extracellular amino termini of GluR3 receptors in nonpermeabilized oocytes showed that membrane insertion of the receptors was directed predominantly to the animal hemisphere. This result raised several questions: where in the vegetal hemisphere are the GFP-tagged proteins located? Why, if their final target is the animal hemisphere, is there a high concentration of GFP-tagged proteins in the vegetal side? Close observation of the vegetal cortex and subcortex revealed that the intracellular fluorescence is localized in patches surrounding cortical granules and elongated structures, which according to their morphology and focal plane localization ≈6 μm, are probably specialized ER substructures detected in early electron-microscope studies of *Xenopus* oocytes (Fig. 1*G*). These structures are now called annulate lamellae (AL) and they are presumed to participate in gene expression and/or mobilization

Table 1. Pharmacological characteristics of WT GluR3 and the GFP-tagged variants

Agonist/antagonist	WT GluR3	GFP-GluR3	GluR3-GFP
Kainate			
EC_{50}	87 ± 6 (6)	129 ± 18 (4)	122 ± 14 (9)
n_H	3 ± 0.2*	1.2 ± 0.1*	1.7 ± 0.1*
Glutamate			
EC_{50}	10 ± 3 (4)	10 ± 2 (6)	78 ± 22 (5)*
n_H	0.8 ± 0.1	1.1 ± 0.2	0.8 ± 0.1
AMPA			
EC_{50}	0.67 ± 0.2 (9)	0.53 ± 0.04 (3)	6.09 ± 1.2 (9)*
n_H	1.3 ± 0.1	1.3 ± 0.2	1.8 ± 0.03*
NBQX (IC_{50})	65 ± 12·10^{-3} (3)	56 ± 12·10^{-3} (4)	59 ± 15·10^{-3} (4)
CNQX (IC_{50})	0.49 ± 0.33 (5)	0.52 ± 0.31 (5)	0.43 ± 0.6 (4)

EC_{50} in μM. Values shown are mean ± SEM. Oocytes were obtained from at least three different donors and injected with at least three different preparations of cRNAs. Number in parentheses is the number of oocytes tested. AMPA was coapplied with CTZ. n_H, slope coefficient. *, $P < 0.05$.

of stored gene products (20). However, the presence of neurotransmitter receptors, either WT or fused with GFP, inside AL has not been described. The intranuclear injection of cDNA coding for the nicotinic α7 subunit fused to GFP produced polarized expression toward the animal hemisphere. No structures containing the α7-GFP proteins were identified (15), perhaps because AL are organelles exclusively situated in the vegetal hemisphere and because the fluorescence in the vegetal hemisphere was relatively low. In the case of GABA ρ1 fused with GFP, the fluorescence was also polarized to the animal hemisphere and the presence of fluorescence in AL was not examined (18). Therefore, the roles played by intracellular organelles and sites of DNA or RNA injection on the paths taken by different receptors and channels from their site of synthesis to the oocyte membrane need further investigation.

Varying the site of GFP tagging to GluR3 led to functional chimeric receptors with different properties. The fusion of GFP to the amino terminus did not alter the properties evaluated in this study and the receptors behaved like the WT. In previous studies, when GFP was tagged to the amino terminus of GluR3 and expressed in HEK 293 cells, the receptors retained their current rectification. However, when expressed in hippocampal neurons in culture the GFP-GluR3 receptors did not reach the synaptic spine membranes. In contrast GFP-GluR1 and GFP-GluR2 chimeras were able to insert into the membrane (28, 29). In our study, tagging GFP to the carboxyl terminus led to receptors that produced larger currents in response to agonist application that were correlated with increases in both fluorescence and amount of protein in the oocyte membrane. Such a positive modulation of the level of expression has not been described for neurotransmitter receptors tagged with GFP. Placing the GFP in the extracellular amino terminus of the hSlo Ca^{2+}-activated K^+ channel reduced its activation by affecting both the voltage and Ca^{2+} dependence of activation (14). In the case of GABAρ1, tagging GFP to the extracellular carboxyl terminus led to slower incorporation of receptors into the plasma membrane and reduced the amplitude of GABA-currents (18). For GluR3 the effects of carboxyl-terminal tagging are complex: there is a decrease in the receptor's sensitivity to glutamate and to AMPA plus CTZ; but there is also an increase in the efficacy due at least partly to reduced receptor desensitization. The slower current decay, together with the increased number of receptors in the membrane, leads to larger agonist responses and counteracts the diminished agonist sensitivity of the GluR3-GFP receptor. It is clear that the GluR3-GFP-currents decay more slowly, but given the Ca^{2+} permeability of GluR3 receptors and the many native Ca^{2+}-activated chloride channels present in the oocyte membrane, more studies are required to decipher the mechanisms responsible for the onset and decay of the Glu currents.

The carboxyl-terminal domain of GluR3 contains several motifs that allow the interaction with numerous signal transduction and scaffolding proteins (30) and are involved in the regulation, traffic and localization of receptor proteins (e.g., ref. 31). Therefore, it is not surprising that inserting GFP in the intracellular terminal domain of the GluR3 receptor alters its properties. However, many further investigations are required to detail the mechanisms involved. It will be of particular interest to determine why inserting GFP close to the presumed agonist binding site apparently does not influence significantly the electrophysiological and pharmacological properties of the receptors.

Our results show that GFP tagging can alter the properties of a receptor, depending on the insertion site. Therefore, extensive functional characterization of the tagged receptor is recommended for proper interpretation of results obtained with tagged receptors. Incidentally, such studies will help to elucidate the structure/function relations of receptors, and GluR3-GFP may be a useful receptor when potentiated AMPA glutamatergic transmission is required.

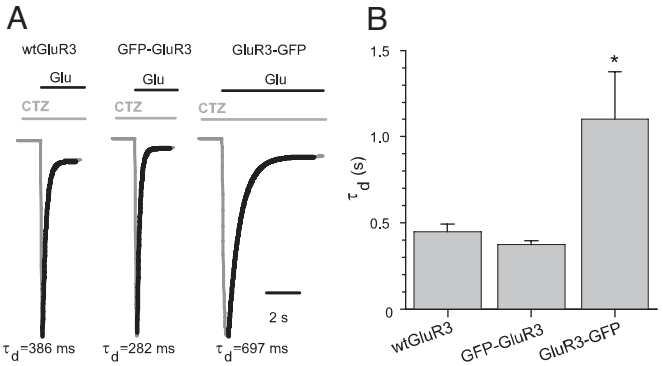

Fig. 6. Carboxyl-terminal GFP tagging alters the decay of GluR3 receptors. (*A*) Glutamate (1 mM) plus CTZ (10 μM)-currents in oocytes injected with GluR3 or the GFP constructs. For better comparison, only the temporal course of activation and decay of the currents are shown. The inactivation was not complete after 20 s of agonist perfusion. After washing out the Glu plus CTZ, the currents returned to their basal level. (*B*) GluR3-GFP-currents decayed more slowly: τ_d = 1,102 ± 276 ms; n = 10; *, $P < 0.05$; vs. WT GluR3 (447 ± 44 ms; n = 10) and GFP-GluR3 (374 ± 20 ms; n = 12). Thicker traces are the exponential fits to the Glu-current traces. Currents were normalized for comparative purposes. Glu-current amplitudes were as follows: 600 nA for WT GluR3, 980 nA for GFP-GluR3, and 3,180 nA for GluR3-GFP.

Materials and Methods

Plasmid DNA Manipulation. Two chimeras were constructed and compared with the GluR3 wild-type receptor (WT GluR3).

GFP-GluR3 has GFP (Clontech, Mountain View, CA) tagged into the amino terminus, inserted between the third and fourth amino acids after the predicted signal peptide cleavage site (7, 28). GluR3-GFP has GFP at the end of the carboxyl terminus. The constructs were assembled in the pBS plasmid (Stratagene, La Jolla, CA) downstream of the T7 promoter. cRNA was produced by linearization of the plasmid (mMessage mMachine kit; Ambion; Austin, TX). Fifty nanoliters of this cRNA (1 mg/ml) were injected into the equatorial band of defolliculated *Xenopus* oocytes and kept in Barth's solution as described previously (32). Expression of GFP-tagged receptors was assessed by confocal microscopy and electrophysiological procedures.

Confocal Microscopy. All Images were obtained by using a Zeiss LSM5 10 META confocal microscope. Expression of the GFP-constructs was evaluated in transverse optical sections taken 300 μm above the oocyte's bottom surface. The fluorescence in the animal and vegetal hemispheres was observed at the same time. For semiquantitative fluorescence analysis of GFP-expressing oocytes, the intensity was measured at the perimeter of the oocyte, and the resultant pixel intensity vs. distance plot was integrated to obtain the area under each profile. To determine the localization of GluR3 receptors inserted in the plasma membrane, a monoclonal antibody (3B3; Zymed Laboratories, San Francisco, CA) raised against the GluR3 amino terminus was used in nonpermeabilized oocytes. Briefly, oocytes were incubated in Barth's solution with 5% FBS, and 0.5% albumin was added for 1 h at room temperature to block unspecific binding. Oocytes were incubated overnight (12°C) in 3 μg/ml of antiGluR3 in Barth's. After washout, oocytes were incubated in Alexa 568-conjugated goat anti-mouse antibody (5 μg/ml) (Invitrogen, Carlsbad, CA) for 1 h at room temperature and finally observed in the confocal.

Western Blot. GluR3 and the GFP-tagged variants were identified in membranes from *Xenopus* oocytes by using two different antibodies. The experiments were done in duplicate. The membrane preparations were made as described (33). Briefly, membrane preparations from eight oocytes were prepared and loaded onto an 8% or 10% SDS polyacrylamide gel (Pierce, Rockford, IL) and separated electrophoretically. Nonspecific binding was blocked by using Tris-buffered saline (TBS) and 5% BSA for 1 h at room temperature. The membranes were incubated for 90 min with the first antibody diluted 1:200 (antiGluR2/3; Chemicon, Hampshire, U.K.) or at 5 μg/ml (antiGluR3), then washed for 45 min with 0.05% Tween 20 in TBS. Secondary antibodies were anti-rabbit or anti-mouse conjugated with alkaline phosphatase, used diluted 1:400. The blots were developed with SigmaFast BCIP/NBT (Sigma, St. Louis, MO).

Electrophysiological Recordings. Two to 6 days after injection, oocytes were impaled with two microelectrodes filled with 3 M KCl and voltage clamped at −80 mV by using a two electrode voltage clamp amplifier (32). Oocytes were placed in a recording chamber and perfused continuously with gravity-driven frog Ringer's solution at room temperature (20–22°C). Kainate, glutamate, and cyclothiazide were purchased from Sigma. NBQX and CNQX and AMPA (*S*-AMPA) were from Tocris Cookson Ltd. (Bristol, U.K.). Currents evoked by agonist perfusion were filtered at 50 Hz and digitized by using NicScope software (34). Agonist concentration-response curves were constructed by measuring the maximum response evoked by each agonist concentration. The agonist concentration causing a half maximal response (EC_{50}) and the slope coefficient (n_H) were estimated for each curve by fitting the data to the logistic type equation (Origin 5.0, Northampton, MA):

$$\text{Amplitude} = \text{maximum amplitude}/(1 + 10^{[\log EC_{50} - \text{Conc of agonist}]n_H})$$

The concentration of NBQX or CNQX causing a decrease to 50% of the 30 μM Kai-current (IC_{50}) was estimated by fitting the following equation to the experimental data:

$$\text{Amplitude} = \text{maximum amplitude}/(1 + 10^{[\text{Conc of agonist} - \log IC_{50}]})$$

The time constant of Glu-current decay (τ_d) was calculated by fitting the equation $I(t) = \exp(-t/\tau_d) + C$, to the decay phase of the current, where I is the current and t is time. Experimental data are shown as mean ± SEM. Differences between two groups were statistically analyzed by Student's t test and considered significant when $P < 0.05$.

We thank Drs. A. Martinez-Torres, Q.-T. Nguyen, and N. C. Spitzer for help with the manuscript. We also thank the American Health Assistance Foundation for support (Grant A2006-054).

1. Ferraguti F, Shigemoto R (2006) *Cell Tissue Res* 326:483–504.
2. Dingledine R, Borges K, Bowie D, Traynelis SF (1999) *Pharmacol Rev* 51:7–61.
3. Jonas P, Burnashev N (1995) *Neuron* 15:987–990.
4. Bennett JA, Dingledine R (1995) *Neuron* 14:373–384.
5. Cull-Candy S, Kelly L, Farrant M (2006) *Curr Opin Neurobiol* 16:288–297.
6. Groc L, Gustafsson B, Hanse E (2006) *Trends Neurosci* 29:132–139.
7. Shi SH, Hayashi Y, Petralia RS, Zaman SH, Wenthold RJ, Svoboda K, Malinow R (1999) *Science* 284:1811–1816.
8. Sheridan DL, Berlot CH, Robert A, Inglis FM, Jakobsdottir KB, Howe JR, Hughes TE (2002) *BMC Neurosci* 3:7.
9. Schaefer H, Rongo C (2006) *Mol Biol Cell* 17:1250–1260.
10. Bueno OF, Robinson LC, Alvarez-Hernandez X, Leidenheimer NJ (1998) *Mol Brain Res* 59:165–177.
11. David-Watine B, Shorte SL, Fucile S, de Saint Jan D, Korn H, Bregestovski P (1999) *Neuropharmacology* 38:785–792.
12. Luo JH, Fu ZY, Losi G, Kim BG, Prybylowski K, Vissel B, Vicini S (2002) *Neuropharmacology* 42:306–318.
13. Diaz LM, Maiya R, Sullivan MA, Han Y, Walton HA, Boehm SL, Bergeson SE, Mayfield RD, Morrisett RA (2004) *J Neurosci Methods* 139:25–31.
14. Meyer E, Fromherz P (1999) *Eur J Neurosci* 11:1105–1108.
15. Palma E, Mileo AM, Martinez-Torres A, Eusebi F, Miledi R (2002) *Proc Natl Acad Sci USA* 99:3950–3955.
16. Fucile S, Palma E, Martinez-Torres A, Miledi R, Eusebi F (2002) *Proc Natl Acad Sci USA* 99:3956–3961.
17. Ikeda M, Beitz E, Kozono D, Guggino WB, Agre P, Yasui M (2002) *J Biol Chem* 277:39873–39879.
18. Martinez-Torres A, Miledi R (2001) *Proc Natl Acad Sci USA* 98:1947–1951.
19. Banke TG, Schousboe A, Pickering DS (1995) *J Neurosci Res* 49:176–185.
20. Kessel RG (1992) *Int Rev Cytol* 133:43–120.
21. Boulter J, Hollmann M, O'Shea-Greenfield A, Hartley M, Deneris E, Maron C, Heinemann S (1990) *Science* 249:1033–1037.
22. Fucile S, Miledi R, Eusebi F (2006) *Proc Natl Acad Sci USA* 103:2943–2947.
23. Kusano K, Miledi R, Stinnakre J (1982) *J Physiol (London)* 328:143–170.
24. Gomez-Hernandez JM, Stühmer W, Parekh AB (1997) *J Physiol (London)* 502:569–574.
25. Peter AB, Schittny JC, Niggli N, Reuter H, Sigel E (1991) *J Cell Biol* 114:455–464.
26. Wild K, Paysan J (2002) *Cell Tissue Res* 307:47–55.
27. Faszewski EE, Kunkel JG (2001) *J Exp Zool* 290:652–661.
28. Shi S, Hayashi Y, Esteban JA, Malinow R (2001) *Cell* 105:331–343.
29. Perestenko PV, Henley JM (2003) *J Biol Chem* 278:43525–43532.
30. Kim E, Sheng M (2004) *Nat Rev Neurosci* 5:771–781.
31. Song I, Huganir RL (2002) *Trends Neurosci* 25:578–588.
32. Miledi R, Parker I, Sumikawa K (1982) *EMBO J* 1:1307–1312.
33. Miledi R, Eusebi F, Martinez-Torres A, Palma E, Trettel F (2002) *Proc Natl Acad Sci USA* 99:13238–13242.
34. Nguyen QT, Miledi R (1995) *J Neurosci Methods* 61:213–219.